Proceedings World Geothermal Congress 2020+1
Reykjavik, Iceland, April - October 2021

An Energy Systems Perspective on the Life Cycle Assessment of Geothermal Heating Networks

Marc Jaxa-Rozen, Astu Sam Pratiwi and Evelina Trutnevyte

Renewable Energy Systems, Institute for Environmental Sciences (ISE), University of Geneva, Switzerland

marc.jaxa-rozen@unige.ch

Keywords: life cycle assessment, sustainability assessment, environmental impacts, ground source heat pumps, district heating

ABSTRACT

The lifespan of new geothermal heating infrastructure can be expected to extend beyond mid-century, likely coinciding with major transitions in the composition of electricity supply to meet greenhouse gas (GHG) targets. However, despite growing interest in the life cycle assessment (LCA) of geothermal heating, there is a lack of knowledge about the environmental impacts associated with geothermal applications with district heating networks powered by large-scale renewable electricity. We thus extend a previously-published LCA study for geothermal heating networks in the State of Geneva, Switzerland. We assess eight environmental impacts for three geothermal design alternatives combining different layouts of district heating network and geothermal extraction temperatures, and for a reference ground-source heat pump (GSHP). We use global sensitivity analysis and scenario discovery to evaluate impacts under uncertainty for eight electricity supply sources, including renewables and fossil fuels. We find that electricity supply source is typically the dominant source of uncertainty in LCA and may lead to trade-offs between impacts: while solar photovoltaic and biomass have low GHG emissions, they respectively lead to the highest water consumption and land use. When compared with GSHP, the relative environmental performance of geothermal heating networks strongly depends on interactions between design parameters of the geothermal network, as well as other energy system properties. Furthermore, different electricity supply technologies may be preferable for different geothermal design configurations. The design of geothermal heating networks should thus account for existing electricity supply, as well as plausible future changes over the lifetime of the system.

1. INTRODUCTION

Life cycle assessment (LCA) has increasingly been applied to study the environmental impacts of geothermal technology. Past studies have largely focused either on Enhanced Geothermal Systems (Pratiwi, Ravier, and Genter 2018) or on geothermal heat pump systems operating under current conditions, for instance, to assess greenhouse gas (GHG) emissions across different country-specific electricity mixes (Marinelli et al. 2019; Saner et al. 2010; Bayer et al. 2012). However, while the environmental impacts of ground-source heat pumps (GSHP) have been well-studied, shallow and medium-depth geothermal applications with district heating networks remain underrepresented in the LCA literature (Pratiwi and Trutnevyte 2021). In particular, there is a lack of knowledge about the environmental impacts which may follow the large-scale integration of renewable electricity with geothermal heating networks, beyond GHG emissions alone. The integration of these energy sources could potentially lead to unexpected impacts and suboptimal "lock-ins", if future changes in electricity supply are not accounted for.

To this end, we study three design alternatives for geothermal heating networks: low-temperature wells with decentralized heat pumps, low-temperature wells with a central heat pump for district heating, and medium-high temperature wells for direct district heating. These design alternatives are based on the LCA model presented in Pratiwi and Trutnevyte (2021). In this conference paper, we conduct a subsequent uncertainty analysis, using global sensitivity analysis and scenario discovery. For each alternative, we sample an ensemble of 18,000 design and operation scenarios by varying 41 uncertain parameters. These uncertainties represent design parameters of the geothermal network, such as production temperature associated with the depth of geothermal well, geothermal flow rate, and the number of geothermal wells. We also consider properties of the broader energy system, such as the generation technology used to supply electricity to the geothermal network, and the share of heating demand that is fulfilled by geothermal heating or auxiliary sources. We include a representative electricity mix for Switzerland, and eight individual electricity generation technologies covering fossil fuels and renewables; we assume auxiliary heating can be provided by waste incineration, natural gas, or electricity. We then use the Ecoinvent 3.5 database (Wernet et al. 2016) and ReCiPe 2016 characterization factors to compute environmental impacts across eight indicators in each scenario: energy consumption, fine particulate matter emissions, fossil and mineral resource scarcity, GHG emissions, land use, soil acidification, and water consumption.

Using these ensembles of scenarios, we identify the uncertain parameters that are most influential towards each environmental impact using global sensitivity analysis. To better understand the potential trade-offs between environmental impacts that are related to the electricity supply source, we then compare the environmental performance of the geothermal configurations with a reference individual ground-source heat pump (GSHP) configuration. As such, we first identify scenarios that are Pareto-efficient across the eight indicators in relation to GSHPs, for each geothermal design alternative and each generation technology separately. We then apply a scenario discovery algorithm to identify the combinations of design parameters and energy system properties that are associated with these Pareto-efficient scenarios. Section 2 details the case study and its computational implementation, followed in Section 3 by results from the sensitivity analysis and trade-off analysis. Section 4 concludes with recommendations for future work.

2. METHODS

2.1 Case study

This case study extends the work of Pratiwi and Trutnevyte (2021), who conducted LCA for six different configurations of geothermal heating and cooling networks, defined as a function of network layout and well depths, across eight environmental impact indicators (Table 1). We combine the six geothermal network configurations of Pratiwi and Trutnevyte (2021) into three design alternatives (Figure 1; detailed parameterizations in appendix, Table A1): a networked heat pump alternative, in which lower-temperature geothermal wells (10°C - 55°C; 10 – 2200m depth) supply a network of connected, decentralized heat pumps; a central heat pump alternative, which uses the same range of geothermal production temperature to supply district heating; and a higher-temperature alternative (78°C - 120°C; 2000 – 4400m depth) for direct district heating. In each alternative, the LCA boundaries include the drilling of geothermal wells, the construction of the heating network, the operation and maintenance of the network over its lifetime, and its decommissioning.

Table 1: Environmental impacts assessed for geothermal heating, using ReCiPe 2016 H characterization factors.

Impact	Description	Unit
Cumulative energy demand	Total life cycle energy used from all sources (including geothermal)	MWh
Fine particulate matter emissions	Emissions of particulate matter with a diameter below 2.5 µm	kg $PM_{2.5}$ eq.
Fossil resource scarcity	Depletion of fossil fuels available for future generations	kg oil eq.
Global warming	Greenhouse gas (GHG) emissions from all sources	kg CO_2 eq.
Land use	Species loss due to the change in land use	$m^2 \cdot yr$ crop eq.
Mineral resource scarcity	Depletion of mineral resources	kg Cu eq.
Terrestrial acidification	Deposition of inorganic substances modifying soil acidity	kg SO_2 eq.
Water consumption	Water consumed over the life cycle, excluding water returned to the water body	m^3

Consistently with previous research (Marinelli et al. 2019), the results of Pratiwi and Trutnevyte (2021) indicated that life cycle impacts were strongly influenced by operational electricity consumption in the case of heat pump-based configurations, in the case of Geneva using a hydropower-based electricity mix. In this work, we test a representative electricity mix based on Swiss national grid supply (Itten, Frischknecht, and Stucki 2014), and eight electricity generation technologies: solar PV, coal, wind power, natural gas, hydropower, nuclear power, biomass, and waste incineration. Datasets used for the Swiss mix and the other technologies are listed in appendix (Table A2). We otherwise maintain the other life cycle inventory assumptions documented in Pratiwi and Trutnevyte (2021) for the geothermal design alternatives, and implement these assumptions using the Ecoinvent 3.5 database (Wernet et al., 2016) and OpenLCA 1.10. We also model a reference GSHP configuration using a representative life cycle inventory included in Ecoinvent 3.5. This configuration assumes a 10 kW brine-water heat pump with a borehole heat exchanger operating at a Seasonal Performance Factor (SPF) of 3.9. We simulate this configuration across the same set of electricity generation technologies and environmental impact indicators. We apply the ReCiPe 2016 H midpoint method (Huijbregts et al., 2017) to quantify each environmental impact, and use a functional unit of 1 MWh of delivered heat.

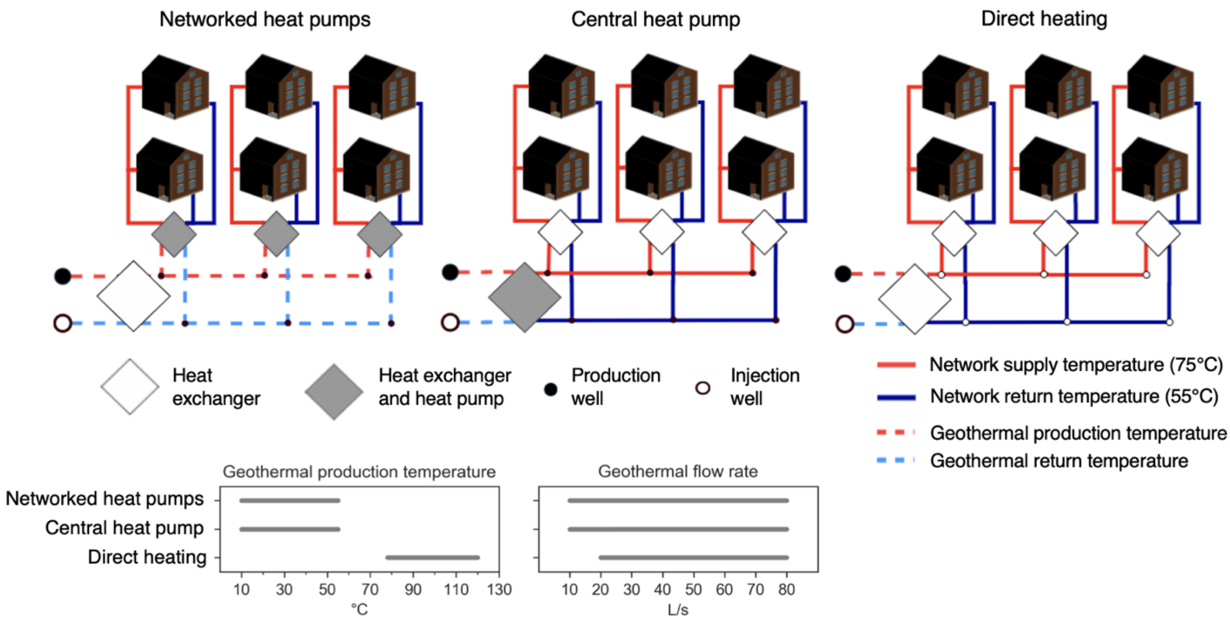

Figure 1: Design alternatives for geothermal heating used in this study (adapted from Pratiwi and Trutnevyte, 2021). Top subplots: heating network design used in each alternative. Bottom subplots: ranges of geothermal production temperature and flow rate in each alternative.

2.2 Computational implementation and analysis

We first sample ensembles of 18,000 scenarios to apply a sensitivity analysis on each geothermal design alternative, using a Latin Hypercube design and assuming independent uniform input distributions on the 41 uncertain input parameters (appendix, Table A1; only 37 parameters are used in the direct heating configuration, which does not use a heat pump). We include the electricity supply source in this sampling. To enable a consistent comparison of relative performance across design alternatives, we use the same quasi-random sampling sequences in all alternatives, and rescale values to each alternative's specific input bounds. For the trade-off analysis, which focuses on the influence of the electricity generation technologies, we separately sample 2,000 scenarios for each of the nine electricity supply sources and each design alternative, again using consistent sampling sequences in each supply source and design alternative. We simulate these scenarios using OpenLCA's Python-based inter-process communication (IPC) interface to parallelize model executions.

We apply the PAWN method for global sensitivity analysis (Pianosi and Wagener 2018), which estimates sensitivity indices for each uncertain input by assessing its impact on the cumulative distribution function (CDF) of the output. This "distribution-based" approach is computationally efficient, and it is more robust than typical variance-based methods for global sensitivity analysis in the case of highly skewed or otherwise non-normal distributions (Borgonovo, Castaings, and Tarantola 2011). We use the SAFE Python package (Noacco et al. 2019) to estimate PAWN indices for each geothermal design alternative, using the Latin Hypercube ensembles. We set 10 conditioning intervals for each uncertain input, and use the median value of the Kolmogorov-Smirnov statistic across these conditioning intervals to define the PAWN median index of each input, averaging over 100 bootstrap resamples. The ranking of sensitivity indices is largely stable for n>8,000 scenarios.

For the trade-off analysis, we use a criterion based on Pareto efficiency (Ravalico, Maier, and Dandy 2009) to identify geothermal heating scenarios that outperform the reference GSHP heating configuration, in each combination of geothermal design alternative and electricity supply source. We consider that a geothermal heating scenario is Pareto-efficient if its environmental impacts are not higher than GSHP on any impact indicator, and lower on at least one impact indicator. We then apply the Patient Rule Induction Method (PRIM) algorithm (Friedman and Fisher 1999; Kwakkel and Jaxa-Rozen 2016) to identify the combinations and ranges of input parameters that characterize each group of Pareto-efficient scenarios. PRIM uses a hill-climbing optimization approach to identify "boxes" of the input uncertainty space which are associated with a given region of the output distribution (in this case, the Pareto-efficient scenarios). The performance of this algorithm is typically described using the notions of coverage and density (Lempert, Bryant, and Bankes 2008), where coverage is the fraction of all scenarios of interest that fall within the box identified by the algorithm, and density is the fraction of scenarios within the box that is of interest. We use the EM Workbench Python package (Kwakkel 2017) to implement the PRIM analysis, and visualize "boxes" meeting a coverage threshold of 75%. The combinations of input parameters identified by the algorithm therefore describe at least this fraction of the total scenarios that are Pareto-efficient in relation to GSHP, for each combination of geothermal design alternative and electricity supply source.

3. RESULTS

3.1 Global sensitivity analysis

The uncertainty analysis yields a broad distribution of outcomes across all eight environmental impacts (Figure 2). Median impacts show a consistent pattern across design alternatives: the highest impacts are obtained with the central heat pump alternative, and the lowest impacts with the direct heating alternative. The relationship between the means and interquartile ranges of the impact distributions indicates that several distributions are highly skewed, for instance in the case of global warming and land use. Using Pearson's r (appendix, Figure A1), we find correlation patterns between environmental impacts that are similar within each design alternative. Fossil resource scarcity and global warming are highly correlated ($r > 0.96$), and cumulative energy demand and fine particulate matter formation are positively correlated with all other impacts. However, land use and mineral resource scarcity in particular are involved in several negative correlations; land use is thus negatively correlated with fossil and mineral resource scarcity, global warming, and water consumption, in both heat pump alternatives. This implies potential trade-offs related to these impacts.

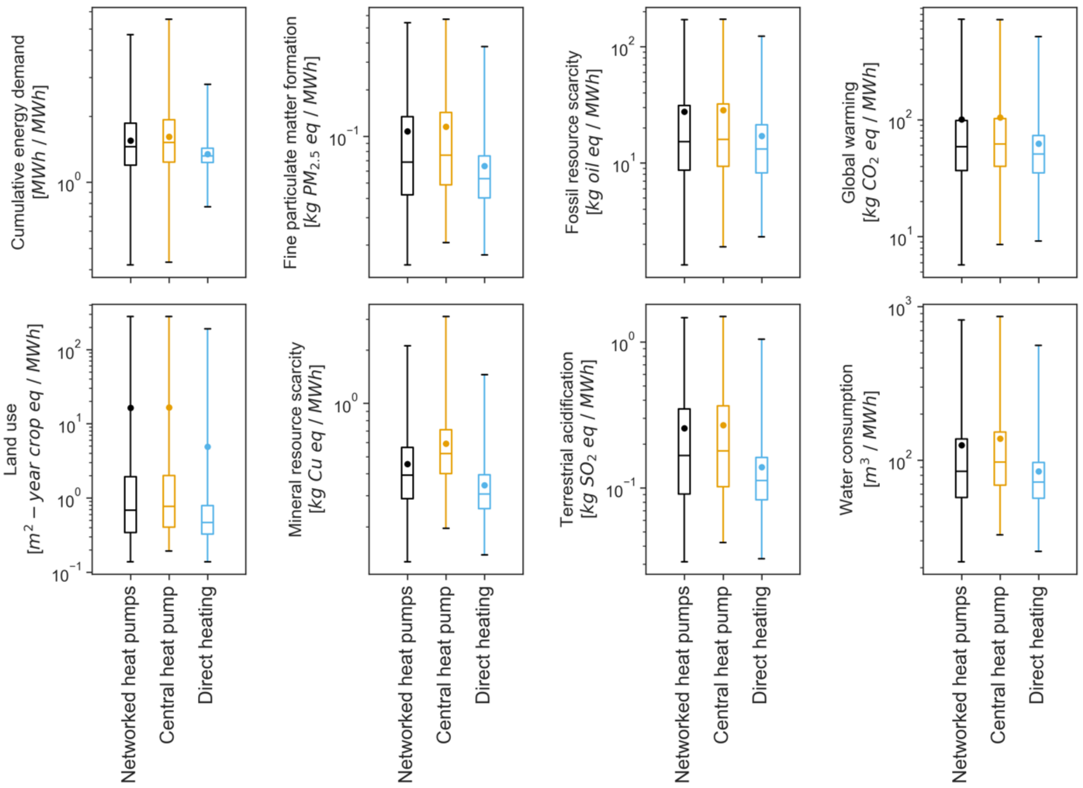

Figure 2: Distribution of environmental impacts, based on separate Latin Hypercube ensembles for each design alternative (*n*=18,000). The ensembles include a random sampling of the nine electricity supply sources in our analysis. For each boxplot, the mean is denoted by a marker, and the median by a horizontal line. Boxes show the interquartile range; whiskers are extended to the full range of the data.

We decompose this uncertainty using PAWN global sensitivity indices (Figure 3), which indicate that the electricity supply source is a key contributor to the uncertainty in impacts. For the heat pump alternatives, it is thus the most influential variable on all environmental impacts. For the direct heating alternative, the share of natural gas in auxiliary heating and the share of geothermal heat are most influential for fossil resource scarcity and global warming, and the district heating linear density is most influential on mineral resource scarcity. Electricity supply nonetheless remains influential towards these impacts. In the absence of the heat pump's contribution to environmental impacts, the influence of other geothermal design parameters emerges more clearly in the direct heating alternative, for instance in the case of geothermal flow rate and well count in relation to fine particulate matter formation and water consumption. Both of these impacts are strongly associated with drilling activities, so that a greater number of wells will consequently lead to higher impacts. However, other uncertainties related to drilling and surface activities, such as transport and disposal distances and exploration well parameters, are relatively non-influential across all impacts and design alternatives.

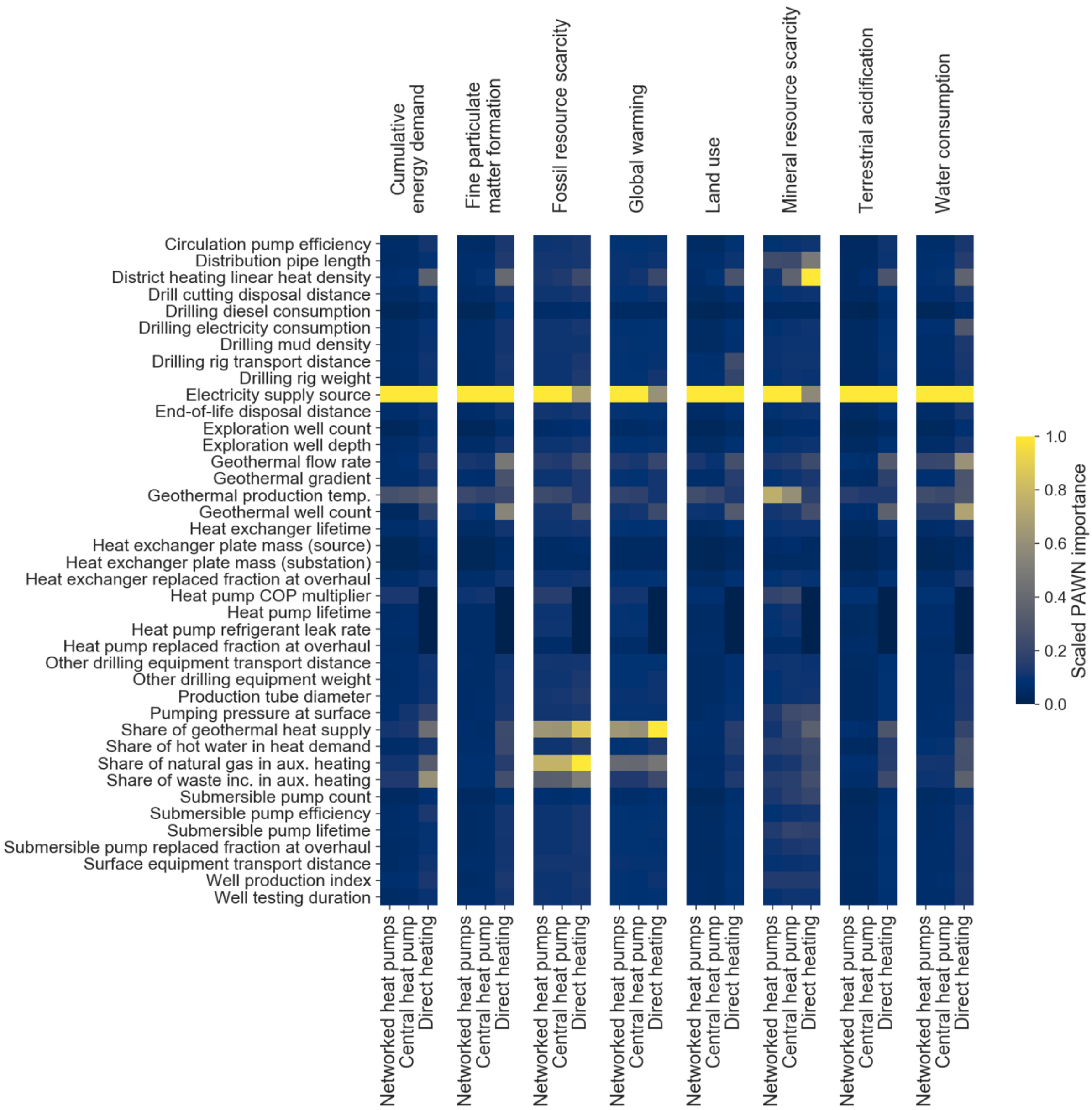

Figure 3: Scaled PAWN sensitivity indices, grouped by environmental impact (subplots) and by design alternative (subplot columns). For each environmental impact, the vector of sensitivity indices is rescaled to [0,1] in each design alternative separately; a value of 1 therefore indicates the parameter with the most influence for each combination of environmental impact and design alternative.

3.2 Trade-off analysis

The influence of electricity supply emerges more clearly in the conditional distribution of impacts across each electricity supply source, for each geothermal design alternative as well as the reference GSHP configuration (Figure 4). Several technologies are associated with significant trade-offs between environmental impacts: biomass-based electricity leads to the highest average impacts on land use, and the second-highest average impacts towards fine particulate matter formation and terrestrial acidification, after coal power. However, it performs relatively well on global warming and fossil resource scarcity. Solar PV and wind power similarly have relatively low average impacts on these two indicators, but have the highest average impacts on mineral resource scarcity. PV furthermore yields the highest average water consumption. Hydropower and waste incineration are associated with the lowest average impacts on all environmental indicators, so that trade-offs between impacts would be less substantial in these cases.

Within each electricity supply source and environmental impact indicator, the design alternative with central heat pump consistently has slightly higher average impacts than the networked heat pump alternative, but the difference is relatively small in relation to the range of impacts. Both of these alternatives uniformly have higher average impacts than the reference GSHP configuration. The relative performance of the direct heating alternative is more variable, which was not apparent in the unconditional distribution of impacts across all electricity supply sources (Figure 2). As such, in combinations of environmental indicators and electricity supply types that are associated with high impacts, such as global warming when using coal or gas, direct heating has the lowest average impacts. Similarly, it has the lowest impacts on water consumption when combined with solar PV, and outperforms GSHP in several cases. However, in several combinations associated with low impacts, such as global warming when using hydropower or waste incineration, direct heating has the highest average impacts. This can likely be explained by the greater impacts of drilling activities for this alternative, which maintain a higher baseline level of impacts in conditions which otherwise minimize operational impacts by using a favorable electricity supply type.

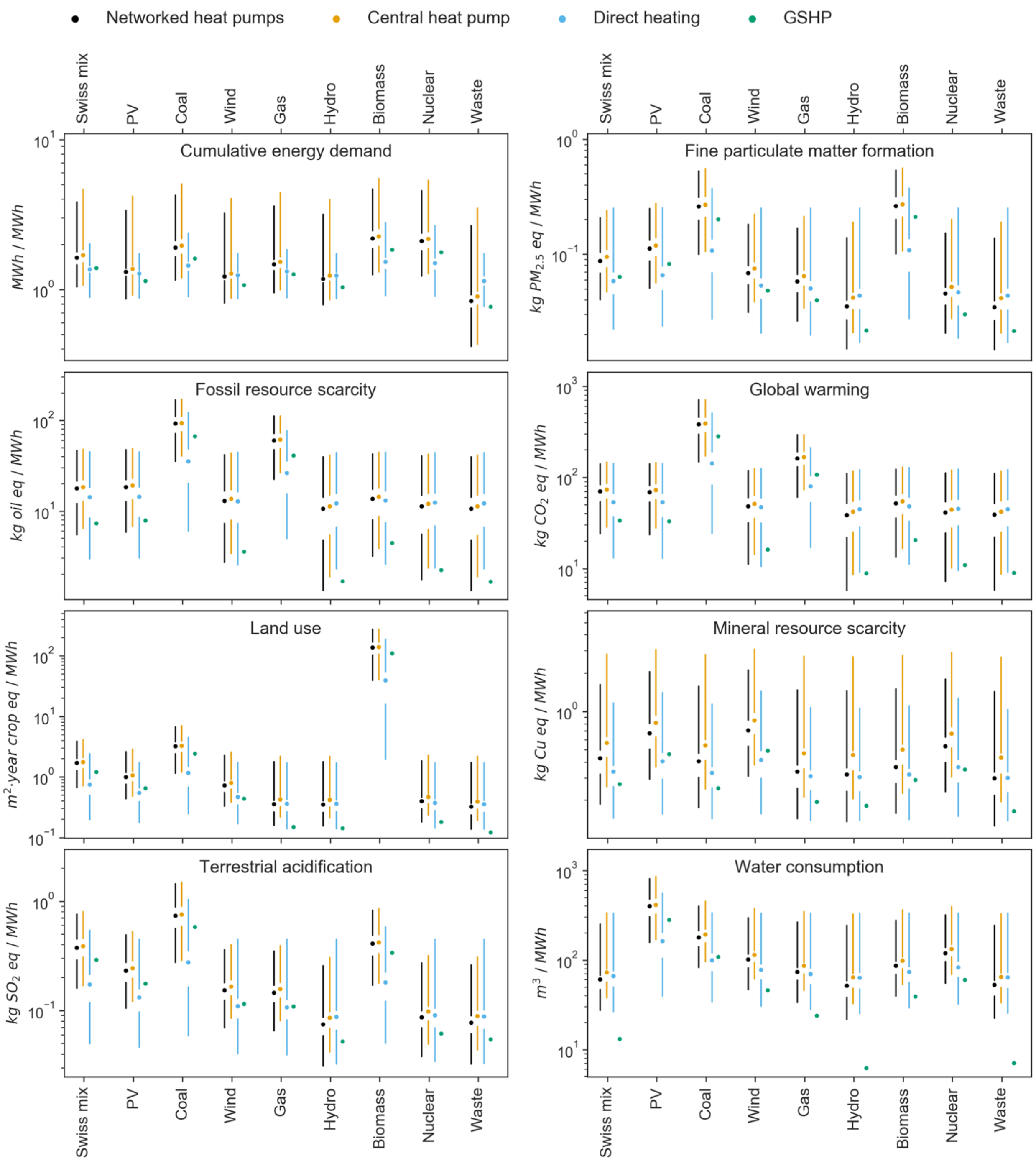

Figure 4: Distribution of environmental impacts grouped by geothermal design alternative and electricity supply source, using separate Latin Hypercube ensembles for each design alternative and supply source (colored lines; *n*=2,000). A green marker shows environmental impacts of the reference ground-source heat pump configuration for each supply source. For each geothermal design alternative, the mean is denoted by a marker; lines are extended to the full range of the data, and line breaks indicate interquartile ranges.

The design alternatives with networked heat pumps or central heat pump consistently have higher average impacts than the reference GSHP configuration, but a significant fraction of scenarios in both alternatives is nonetheless Pareto-efficient relative to GSHP (Figure 5). In all combinations of geothermal design alternatives and electricity supply sources, multiple individual scenarios thus outperform GSHP on at least one of the environmental impact indicators. Interestingly, electricity supply technologies lead to different patterns of relative performance across the geothermal design alternatives: using waste incineration, 40% of scenarios are Pareto-efficient with the networked heat pump alternative. However, only 9% are Pareto-efficient with the direct heating alternative, which otherwise performs well using the other supply technologies, except hydropower. Biomass-based electricity is the most favorable in terms of Pareto-efficiency for all geothermal design alternatives, as the high land use impacts caused by this technology also affect the GSHP configuration. Hydropower is less favorable for the geothermal design alternatives as compared to GSHP, yielding the lowest fraction of Pareto-efficient scenarios in the networked and central heat pump alternatives (22% and 9.6%), and the second-lowest fraction for direct heating (12%).

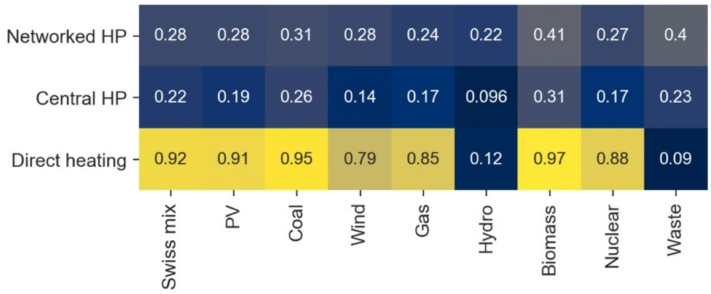

Figure 5: Fraction of scenarios that are Pareto-efficient relative to the reference ground-source heat pump configuration, for each combination of geothermal design alternative and electricity supply source (*n*=2,000 in each combination).

3.3 Scenario discovery

We complete the analysis by identifying the combinations of input parameters associated with these Pareto-efficient scenarios for a subset of electricity supply technologies (Figure 6). We illustrate wind and natural gas as examples of renewable and fossil energy sources, as well as hydropower and waste incineration, due to their different pattern of relative performance across geothermal alternatives. For the networked heat pump alternative, a minimum threshold for geothermal production temperature is retained by PRIM as a key factor using any of the four electricity supply technologies, in combination with other variables. For example, using wind power, the Pareto-efficient scenarios are associated with a production temperature greater than 37°C, combined with a heat pump COP multiplier greater than 0.34, and with an auxiliary heating share of at least 17% for waste incineration (note that the COP multiplier here corresponds to the ratio of real COP to ideal COP). A similar combination of parameters is identified for the case of natural gas generation. Using hydropower, which is the least favorable for this geothermal alternative, Pareto-efficient scenarios additionally require a relatively greater flow rate (>20 l/s), and an auxiliary heating share below 39% for natural gas. Conversely, using waste incineration, which is the most favorable electricity supply technology, Pareto-efficient scenarios are only restricted in relation to production temperature (>20°C) and auxiliary gas heating share (<30%, with residual demand indifferently supplied by geothermal heat, heat from waste incineration, or electric heating generated from the latter).

For the central heat pump alternative, Pareto-efficient scenarios are similarly driven by interactions between electricity supply technologies and geothermal system design, with a minimum linear heat density for the district heating network being significant when using wind power or gas generation (>2 and >1.1 MWh/(yr·m), respectively). Geothermal production temperature is also restricted to a relatively high range in the case of wind power, gas generation, and hydropower (>31°C, >32°C, >25°C, respectively). We note that in the case of waste incineration, the share of geothermal heat in total supply is constrained to a maximum of 91%, in combination with an auxiliary gas heating share below 29%: Pareto-efficient scenarios thus leave a greater share for auxiliary heat from waste incineration, and/or electric heating generated from waste incineration, rather than geothermal heating.

In the case of direct heating, a minimum threshold for linear heat density is retained for all four electricity sources; this parameter was previously identified as highly influential towards mineral resource scarcity in particular. For wind power or gas generation, using which geothermal heating is Pareto-efficient in a large majority of scenarios, linear heat density is only lightly restricted (>1.7 and >0.83 MWh/(yr·m), respectively), in combination with a wide range of geothermal heat share. However, using hydropower or waste incineration, with which GSHP typically outperforms geothermal heating, Pareto-efficient scenarios require a relatively high linear heat density (>2.7 and >2.9 MWh/(yr·m)), accompanied by a relatively high geothermal flow rate (>29 and >37 l/s), and a smaller number of wells (≤ 3). The latter parameter logically reduces impacts associated with drilling, which were a significant contributor to life cycle impacts in Pratiwi and Trutnevyte (2021).

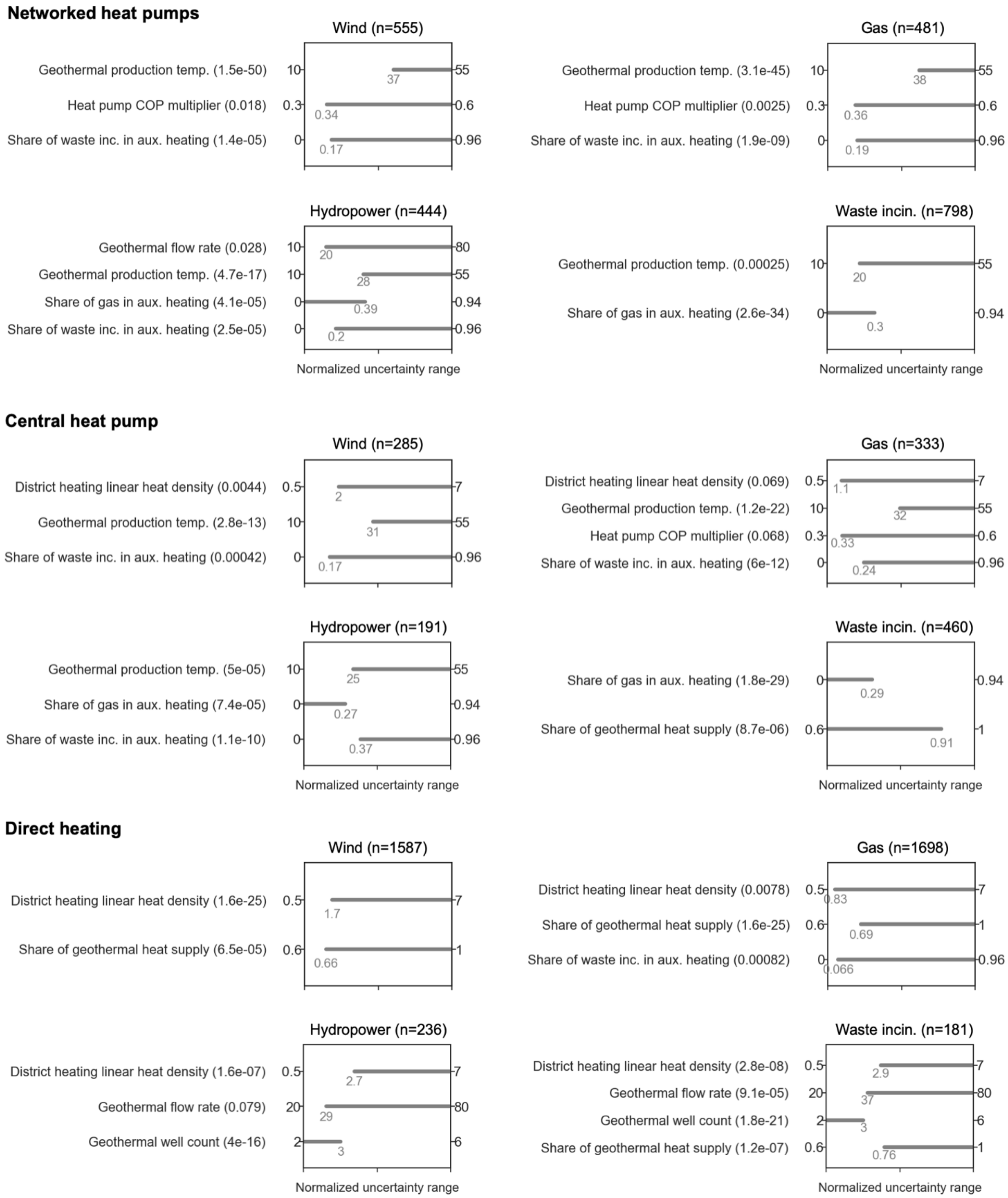

Figure 6: Uncertainty ranges associated with Pareto-efficient scenarios relative to GSHP for each geothermal design alternative, identified using PRIM at a coverage threshold of 75%, using four electricity supply technologies. Normalized uncertainty ranges show the full range of input uncertainties sampled in the Latin Hypercube ensemble for each combination of geothermal design alternative and electricity supply technology (*n*=2,000). Gray lines show the restricted range of each input found to be significant (*p*<0.1) for each technology. Estimated p-values for the significance of each restriction are shown in parenthesis.

4. CONCLUSIONS

Our results generally support previous findings in relation to the strong influence of electricity supply on the life cycle impacts of geothermal heating. For heat pump-based geothermal design alternatives, the electricity generation technology is thus the dominant source of uncertainty in all eight impacts considered in our study, and in five impacts in the case of direct geothermal heating. Overall, electricity generated by hydropower or waste incineration yields the lowest environmental impacts across the three geothermal network configurations. However, certain technologies are associated with significant trade-offs between the environmental indicators: solar PV yields low GHG emissions, but causes the highest impacts on water consumption, whereas biomass-based power similarly performs well on GHG emissions, but leads to the highest impacts on land use.

When compared to reference GSHP heating systems using the same set of electricity generation technologies, we find that the relative environmental performance of geothermal heating is strongly dependent on the design parameters, such as geothermal production temperature, and on other energy system properties, such as the linear heat density of district heating. The electricity generation technology influences the ranges of these parameters that yield favorable relative performance for geothermal heating. For instance, in the case of geothermal heating with networked heat pumps, systems powered by hydropower need a relatively strict combination of design parameters and auxiliary heating properties to be Pareto-efficient relative to GSHP, while systems powered by waste incineration are more robust on this measure.

Furthermore, different electricity supply technologies may be preferable for different geothermal design configurations. Under the assumptions used in our analysis, direct geothermal heating generally displayed the most robust environmental performance in relation to electricity supply, while heat pump-based design alternatives were logically more sensitive to this uncertainty, given the importance of operational electricity consumption in life cycle impacts. However, in the case of systems powered by hydropower or waste incineration, the networked heat pump design alternative offered the most robust performance relative to GSHP. The selection of a geothermal design configuration and its parameterization should thus account for local electricity supply conditions, as well as plausible changes in future electricity supply over the lifetime of the system. These results underline the importance of a systemic perspective on the integration of large-scale renewable generation and geothermal heating, which may otherwise affect the relative environmental performance of the latter, and yield unexpected trade-offs with environmental impacts left out of the scope of a GHG-focused analysis.

REFERENCES

Bayer, Peter, Dominik Saner, Stephan Bolay, Ladislaus Rybach, and Philipp Blum. 2012. “Greenhouse Gas Emission Savings of Ground Source Heat Pump Systems in Europe: A Review.” *Renewable and Sustainable Energy Reviews* 16 (2): 1256–67. https://doi.org/10.1016/j.rser.2011.09.027.

Borgonovo, E., W. Castaings, and S. Tarantola. 2011. “Moment Independent Importance Measures: New Results and Analytical Test Cases.” *Risk Analysis* 31 (3): 404–28. https://doi.org/10.1111/j.1539-6924.2010.01519.x.

Friedman, Jerome H., and Nicholas I. Fisher. 1999. “Bump Hunting in High-Dimensional Data.” *Statistics and Computing* 9 (2): 123–43. https://doi.org/10.1023/A:1008894516817.

Itten, R., R. Frischknecht, and M. Stucki. 2014. “Life Cycle Inventories of Electricity Mixes and Grid.” Version 1.3. Uster, Switzerland: treeze Ltd.

Kwakkel, Jan H. 2017. “The Exploratory Modeling Workbench: An Open Source Toolkit for Exploratory Modeling, Scenario Discovery, and (Multi-Objective) Robust Decision Making.” *Environmental Modelling & Software* 96: 239–250.

Kwakkel, Jan H., and Marc Jaxa-Rozen. 2016. “Improving Scenario Discovery for Handling Heterogeneous Uncertainties and Multinomial Classified Outcomes.” *Environmental Modelling & Software* 79 (May): 311–21. https://doi.org/10.1016/j.envsoft.2015.11.020.

Lempert, Robert, Benjamin Bryant, and Steven Bankes. 2008. “Comparing Algorithms for Scenario Discovery.” WR-557-NSF. Santa Monica, CA: RAND Corporation.

Marinelli, Simona, Francesco Lolli, Rita Gamberini, and Bianca Rimini. 2019. “Life Cycle Thinking (LCT) Applied to Residential Heat Pump Systems: A Critical Review.” *Energy and Buildings* 185 (February): 210–23. https://doi.org/10.1016/j.enbuild.2018.12.035.

Noacco, Valentina, Fanny Sarrazin, Francesca Pianosi, and Thorsten Wagener. 2019. “Matlab/R Workflows to Assess Critical Choices in Global Sensitivity Analysis Using the SAFE Toolbox.” *MethodsX* 6: 2258–2280.

Pianosi, Francesca, and Thorsten Wagener. 2018. “Distribution-Based Sensitivity Analysis from a Generic Input-Output Sample.” *Environmental Modelling & Software* 108 (October): 197–207. https://doi.org/10.1016/j.envsoft.2018.07.019.

Pratiwi, Astu Sam, Guillaume Ravier, and Albert Genter. 2018. “Life-Cycle Climate-Change Impact Assessment of Enhanced Geothermal System Plants in the Upper Rhine Valley.” *Geothermics* 75 (September): 26–39. https://doi.org/10.1016/j.geothermics.2018.03.012.

Pratiwi, Astu Sam, and Evelina Trutnevyte. 2021. “Life Cycle Assessment of Shallow to Medium-Depth Geothermal Heating and Cooling Networks in the State of Geneva.” *Geothermics* 90 (February): 101988. https://doi.org/10.1016/j.geothermics.2020.101988.

Ravalico, Jakin K., Holger R. Maier, and Graeme C. Dandy. 2009. “Sensitivity Analysis for Decision-Making Using the MORE Method—A Pareto Approach.” *Reliability Engineering & System Safety*, Special Issue on Sensitivity Analysis, 94 (7): 1229–37. https://doi.org/10.1016/j.ress.2009.01.009.

Saner, Dominik, Ronnie Juraske, Markus Kübert, Philipp Blum, Stefanie Hellweg, and Peter Bayer. 2010. “Is It Only CO2 That Matters? A Life Cycle Perspective on Shallow Geothermal Systems.” *Renewable and Sustainable Energy Reviews* 14 (7): 1798–1813. https://doi.org/10.1016/j.rser.2010.04.002.

Wernet, Gregor, Christian Bauer, Bernhard Steubing, Jürgen Reinhard, Emilia Moreno-Ruiz, and Bo Weidema. 2016. “The Ecoinvent Database Version 3 (Part I): Overview and Methodology.” *The International Journal of Life Cycle Assessment* 21 (9): 1218–30. https://doi.org/10.1007/s11367-016-1087-8.

APPENDIX

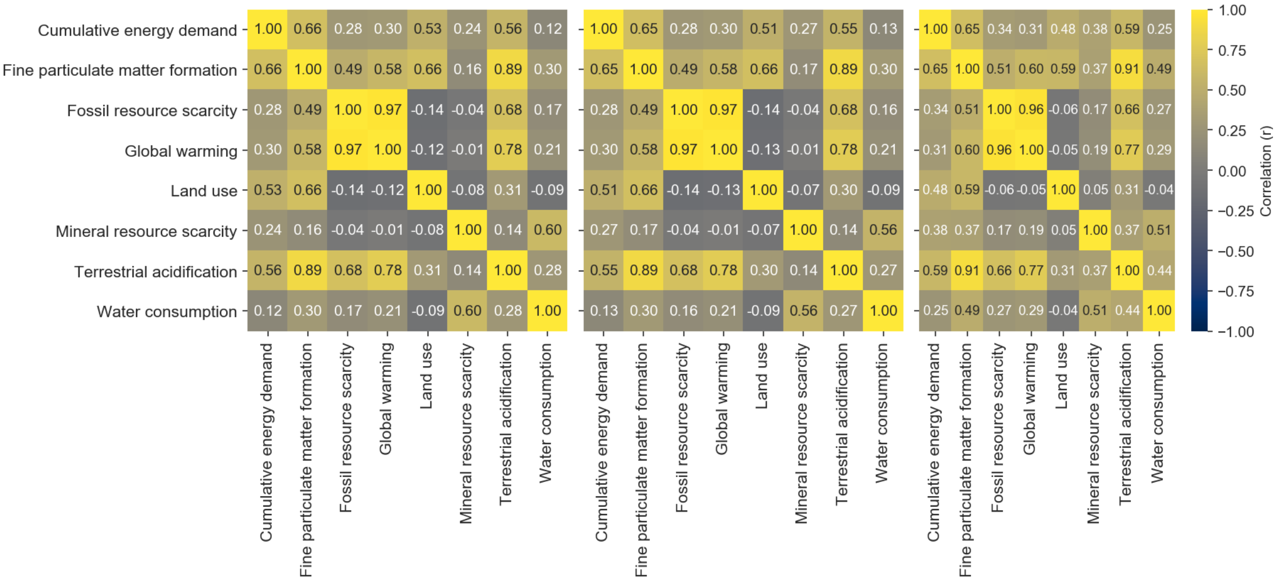

Figure A1: Correlation between environmental impacts (Pearson’s *r*), using Latin Hypercube ensembles (n=18,000). Left panel: networked heat pump alternative; middle panel: central heat pump alternative; right panel: direct heating alternative.

Table A1: Uncertain parameters used in the analysis. A uniform distribution is used for all bounds except where noted.

Parameter	Unit	Design alternative		
		Networked heat pumps	**Central heat pump**	**Direct heating**
Circulation pump efficiency	-	0.5 - 0.9	0.5 - 0.9	0.5 - 0.9
Distribution pipe length	m	100 - 2000	100 - 2000	100 - 2000
District heating linear heat density	MWh/(yr·m)	0.5 - 0.7	0.5 - 7	0.5 - 7
Drill cutting disposal distance	km	5 - 200	5 - 200	5 - 200
Drilling diesel consumption [1]	GJ/m	{Low, medium, high}		
Drilling electricity consumption	MWh/m	0.02 - 0.1	0.02 - 0.1	0.02 - 0.1
Drilling mud density	kg/m	0.05 - 55	0.05 - 55	45 - 55
Drilling rig mobilization distance	km	100 - 1000	100 - 1000	100 - 1000
Drilling rig weight [1]	t	{Low, medium, high}		
Electricity supply source [2]		{Swiss mix, PV, Coal, Wind, Gas, Hydropower, Biomass, Nuclear, Waste incineration}		
End-of-life disposal distance	km	20 - 100	20 - 100	20 - 100
Exploration well count	integer	1 - 4	1 - 4	1 - 4
Exploration well depth	m	50 - 150	50 - 150	150 - 250
Geothermal flow rate	l/s	10 - 80	10 - 80	20 - 80
Geothermal gradient	°C/m	0.02 - 0.035	0.02 - 0.035	0.02 - 0.035
Geothermal production temp.	°C	10 - 55	10 - 55	78 - 120
Geothermal well count	integer	2 - 6	2 - 6	2 - 6
Heat exchanger lifetime	year	5 - 30	5 - 30	5 - 30
Heat exchanger plate mass (source) [3]	kg	{0.0322(P [kW])+15.57, 0.1053(P[kW])+9.8, 0.0284(P[kW])+1.581}		
Heat exchanger plate mass (substation) [3]	kg	{0.0322(P [kW])+15.57, 0.1053(P[kW])+9.8, 0.0284(P[kW])+1.581}		
Heat exchanger replaced fraction at overhaul	-	0.3 - 0.9	0.3 - 0.9	0.3 - 0.9
Heat pump COP multiplier	1/ideal COP	0.3 - 0.6	0.3 - 0.6	-
Heat pump lifetime	year	10 - 20	10 - 20	-
Heat pump refrigerant leak rate	-	0.02 - 0.1	0.02 - 0.1	-
Heat pump replaced fraction at overhaul	-	0.3 - 0.9	0.3 - 0.9	-
Other drilling equipment transport distance	km	100 - 1000	100 - 1000	100 - 1000
Other drilling equipment weight	t	20 - 200	20 - 200	20 - 200

Production tube diameter	in	4 - 9	4 - 9	6 - 8
Pumping pressure at surface	bar	1 - 11	1 - 11	1 - 25
Share of geothermal heat supply [4]	-	0.6 - 1	0.6 - 1	0.6 - 1
Share of domestic hot water in heat demand	-	0.2 - 0.4	0.2 - 0.4	0.2 - 0.4
Share of natural gas in aux. heating [4]	-	0.02 - 0.96	0.02 - 0.96	0.02 - 0.96
Share of waste inc. in aux. heating [4]	-	0.02 - 0.96	0.02 - 0.96	0.02 - 0.96
Submersible pump count	integer	1 - 6	1 - 6	1 - 6
Submersible pump efficiency	-	0.5 - 0.7	0.5 - 0.7	0.5 - 0.7
Submersible pump lifetime	year	5 - 20	5 - 20	5 - 20
Submersible pump replaced fraction at overhaul	-	0.3 - 0.9	0.3 - 0.9	0.3 - 0.9
Surface equipment transport distance	km	30 - 1000	30 - 1000	30 - 1000
Well production index	-	2 - 10	2 - 10	2 - 10
Well testing duration	day	10 - 100	10 - 100	10 - 100

[1] Depth-dependent relationship - see Table A.6 in Pratiwi and Trutnevyte (2021)

[2] Detailed in Table A2.

[3] The heat exchanger plate mass is computed as a function of thermal power using one of the randomly sampled relationships.

[4] The total annual heat supply is decomposed in fractional shares *S* of geothermal heat and auxiliary heat, with auxiliary heat provided by gas, waste, or electric heating: $S_{aux} = 1 - S_{geo} = S_{gas} + S_{waste} + S_{elec}$. The shares of the three auxiliary sources are Gamma-distributed with a shape parameter k=1.3 and scale parameter θ=0.3 within the specified bounds.

Table A2: Definition of the electricity supply sources used in the analysis.

Source	Share	Ecoinvent 3.5 dataset
Swiss mix [1,2,3]	0.208	electricity production, hydro, reservoir, alpine region | electricity, high voltage | Cutoff, U - CH
	0.188	electricity production, hydro, run-of-river | electricity, high voltage | Cutoff, U - CH
	0.134	electricity production, nuclear, pressure water reactor | electricity, high voltage | Cutoff, U - CH
	0.121	electricity production, nuclear, boiling water reactor | electricity, high voltage | Cutoff, U - CH
	0.087	electricity, high voltage, import from DE | electricity, high voltage | Cutoff, U - CH
	0.075	electricity, high voltage, import from FR | electricity, high voltage | Cutoff, U - CH
	0.061	electricity, high voltage, hydro, run-of-river, import from France | electricity, high voltage | Cutoff, U - CH
	0.043	electricity, high voltage, import from AT | electricity, high voltage | Cutoff, U - CH
	0.035	electricity, high voltage, nuclear, import from France | electricity, high voltage | Cutoff, U - CH
	0.030	market for electricity, high voltage | electricity, high voltage | Cutoff, U - CH
	0.014	heat and power co-generation, biogas, gas engine | electricity, high voltage | Cutoff, U - CH
	0.012	electricity, high voltage, hydro, reservoir, import from France | electricity, high voltage | Cutoff, U - CH
Solar PV [3]	0.722	electricity production, PV, 3kWp slanted-roof installation, single-Si, panel, mounted | electricity, low voltage | Cutoff, U - CH
	0.095	electricity production, PV, 3kWp slanted-roof installation, multi-Si, panel, mounted | electricity, low voltage | Cutoff, U - CH
	0.037	electricity production, PV, 3kWp flat-roof installation, multi-Si | electricity, low voltage | Cutoff, U - CH
	0.024	electricity production, PV, 3kWp flat-roof installation, single-Si | electricity, low voltage | Cutoff, U - CH
	0.023	electricity production, PV, 3kWp slanted-roof installation, CdTe, laminated, integrated | electricity, low voltage | Cutoff, U - CH
	0.021	electricity production, PV, 3kWp slanted-roof installation, a-Si, panel, mounted | electricity, low voltage | Cutoff, U - CH
	0.013	electricity production, PV, 3kWp slanted-roof installation, ribbon-Si, panel, mounted | electricity, low voltage | Cutoff, U - CH
	0.012	electricity production, PV, 3kWp slanted-roof installation, multi-Si, laminated, integrated | electricity, low voltage | Cutoff, U - CH
	0.012	electricity production, PV, 3kWp facade installation, multi-Si, panel, mounted | electricity, low voltage | Cutoff, U - CH
	0.012	electricity production, PV, 3kWp facade installation, multi-Si, laminated, integrated | electricity, low voltage | Cutoff, U - CH
	0.008	electricity production, PV, 3kWp facade installation, single-Si, laminated, integrated | electricity, low voltage | Cutoff, U - CH
	0.008	electricity production, PV, 3kWp facade installation, single-Si, panel, mounted | electricity, low voltage | Cutoff, U - CH
	0.008	electricity production, PV, 3kWp slanted-roof installation, single-Si, laminated, integrated | electricity, low voltage | Cutoff, U - CH
Coal [1,2,3]	-	electricity production, hard coal | electricity, high voltage | Cutoff, S - DE
Wind power [1,2,3]	-	electricity production, wind, >3MW turbine, onshore | electricity, high voltage | Cutoff, S - CH
Natural gas [1,2,3]	-	electricity production, natural gas, combined cycle power plant | electricity, high voltage | Cutoff, S - CH
Hydropower [1,2,3]	-	electricity production, hydro, run-of-river, label-certified | electricity, high voltage, label-certified | Cutoff, U - CH
Biomass [1,2,3]	-	heat and power co-generation, wood chips, 6667 kW | electricity, high voltage | Cutoff, S - CH
Nuclear [1,2,3]	-	electricity production, nuclear, boiling water reactor | electricity, high voltage | Cutoff, S - CH
Waste incineration [2,3]	-	electricity, from municipal waste incineration to generic market for electricity, med. voltage | electricity, med. voltage | Cutoff, S - CH

For each supply source, superscripts indicate datasets used to model transmission and distribution, based on Pratiwi and Trutnevyte (2021):

Identifier	Ecoinvent 3.5 dataset	Amount
1	Transmission network, electricity, high voltage	6×10^{-6} km/MWh
2	Transmission network, electricity, medium voltage	1.86×10^{-5} km/MWh
3	Distribution network, electricity, low voltage	8.7×10^{-5} km/MWh